International Journal of Heat and Mass Transfer 54 (2011) 3323–3333

Contents lists available at ScienceDirect

International Journal of Heat and Mass Transfer

journal homepage: www.elsevier.com/locate/ijhmt

Heat transfer from small objects in microgravity: Experiments and analysis

Margaritis Kostoglou, Sotiris P. Evgenidis, Konstantinos A. Zacharias, Thodoris D. Karapantsios *

Division of Chemical Technology, School of Chemistry, Aristotle University, University Box 116, 541 24 Thessaloniki, Greece

ARTICLE INFO

Article history:
Received 29 October 2009
Accepted 24 March 2011
Available online 27 April 2011

Keywords:
Natural convection
Microgravity
Conduction
Rayleigh number
Spheroidal thermistor

ABSTRACT

Heat transfer over a sub-millimeter spheroidal solid is of interest in many engineering processes. One important mechanism of heat transfer in the above processes is natural convection which leads to heat transfer rates many times larger than that of pure conduction. Despite the huge literature devoted to natural convection heat transfer rates over spheres (and to a smaller extent over spheroids) there is not a generally accepted correlation especially for small Rayleigh numbers. Existing correlations for external geometries predict a progressively increasing contribution of natural convection to heat transfer with respect to gravity (starting from zero gravity). To test the validity of these correlations, experiments are performed for the estimation of heat transfer rates at low gravity. Heat pulses are given to a miniature thermistor with a nearly spheroidal shape immersed in a liquid and its thermal response is registered during heating in parabolic flights. The contribution of natural convection to heat transfer is undoubtedly estimated from runs in which acceleration varies from 0 to 1.8 g. Surprisingly enough, the experiments showed that the Rayleigh number must take a minimum value before non-negligible effect of natural convection on heat transfer appears (existence of a threshold Rayleigh number). In the absence of natural convection (below Ra_{thr}) the experimental thermal response curves can be successfully described by approximating solutions of the transient heat conduction equation for the spheroidal geometry of the thermistor. Apparently, additional research is needed regarding the natural convection around sub-millimeter objects for small Rayleigh numbers.

1. Introduction

Natural convection over a small spherical (or approximately spherical) object is of interest in many engineering processes such as manufacturing systems, heat transfer in packed beds and for many electronic components of nearly spherical shape [1]. This is the reason of the very extensive theoretical and experimental study of the problem during the last 60 years. This particular problem is dictated by the Grashof (Gr) or equivalently by the Rayleigh number (Ra = GrPr where Pr is the Prandtl number). Both numbers express the ratio of buoyancy induced convective transport to transport by molecular means (momentum transport for Gr and heat transport for Ra). The mathematical problem which must be solved consists of the momentum and heat transfer equations. The motion is induced by a momentum source term emerging from the temperature dependence of the fluid density.

Several simplifications can be made to the mathematical problem at steady and pseudo-steady state. The so-called Boussinesq approximation is usually employed to transform the system of equations to a linear one which can be handled easier [2]. The main assumption of Boussinesq approximation is to neglect the temperature dependence of fluid properties except that of density which is assumed to exhibit linear temperature dependence. This approximation is often applied outside the limits of its validity, e.g., if the fluid's viscosity is strongly depended on temperature.

Another simplification has to do with the limit of large Grashof number [3]. In this limit, the thickness of the layer in which fluid motion and heat transfer take place is small with respect to its length so a boundary layer approximation can be applied replacing the elliptic problem with an easier to solve parabolic one. This type of simplification is used for axisymmetric objects of any shape since in this limit the boundary layer thickness is much smaller than the radius of curvature, so curvature can be ignored [4].

Another approximate technique leading to analytical results in case of spheres have been employed for the limit of small Grashof number [5,6]. A perturbation expansion with respect to Grashof number is not everywhere valid since far from the sphere the convection and conduction terms are of the same magnitude. Different expansions are needed at different regions followed by a matching procedure to get the final result.

Regarding transient natural convection, a step change in the object temperature is the scenario mostly studied. Analytical results for the cases of small Grashof number are given in [7]. Another important case of transient natural convection is the so-called

* Corresponding author. Tel./fax: +30 2310997772.
E-mail address: karapant@chem.auth.gr (T.D. Karapantsios).

0017-9310/$ - see front matter © 2011 Elsevier Ltd. All rights reserved.
doi:10.1016/j.ijheatmasstransfer.2011.03.053

Nomenclature

A	heat transfer surface area
A_s	surface area of the spheroidal thermistor
c_p	specific heat capacity
g	gravitational acceleration on earth
H	ratio of natural convection to conduction contribution to heat transfer
I	electric current in the thermistor network
K	thermal conductivity
k_l	thermal conductivity of the liquid
k_m	thermal conductivity of the metallic part of the thermistor
k_q	thermal conductivity of the quartz
P	heating power of the thermistor
Q_R	heat transfer rate from a sphere to the environment through conduction
Q_{Rs}	steady state heat transfer rate from a sphere to its environment through conduction
Q_{ss}	steady state heat transfer rate from a spheroid to its environment through conduction
r	radial coordinate
R_1	reference resistance used by the thermistor
R_s	equivalent radius of the thermistor
R_t	internal resistance of thermistor
R	radius of a spherical heat source
S_1, S_2	interfaces between domains defined in Fig. 1
t	time
T_c	characteristic temperature for physical properties computation
T_f	film temperature defined as $(T_o + T_t)/2$
T_i	outer thermistor temperature (quartz-liquid interface)
T_o	initial and far-field fluid temperature
T_t	temperature of the thermistor
V_1, V_2, V_3, V_4	domains of the problem defined in Fig. 1
V_o	voltage applied to the thermistor
V_R	voltage difference at the edges of R_t
V_s, ρ_s, c_{ps}	volume, density and specific heat capacity of the metallic part of the thermistor
α, b	length of large and small spheroidal thermistor semiaxis
α_q	thermal diffusivity of the quartz
α_w	thermal diffusivity of the liquid
β	liquid thermal expansion coefficient
γ	gravitational acceleration
δ	thickness of the quartz layer
μ	liquid viscosity
ρ	density

gravity modulation or g-jitter induced flow in reduced gravity environments. Small accelerations (g-jitters) are due to crew motions, mechanical vibrations, atmospheric drag, earth gravity gradient and other sources. Although in practice they are of stochastic nature, they are typically modeled as high frequency harmonic functions [8,9]. The above approximate analytical results combined with experimental results have led to the development of several correlations in literature for heat transfer around spheres and spheroids [10]. According to these correlations natural convection emerges even in the case of g-jitters.

The study of the effect of g-jitters on heat transfer and particularly on natural convection is the primary objective of the present study. This is important in order to assess the significance of natural convection which is usually assumed negligible in parabolic flights [11,12]. The structure of the work is the following: First, the experimental set-up and the experimental procedure are described. Then, the collected data are presented in a comprehensive form. A discussion is made about the existence or not of natural convection in each experiment. Adopting a mechanistic thermal engineering point of view, we do not assign the term natural convection in the present work to the motion of fluid due to buoyancy (undetectable by the present experimental means) but to the heat transfer effect of buoyancy which can be experimentally detected. So, the claimed absence of natural convection may refer to weak fluid motion with non-measurable effect on heat transfer. Data are analyzed and discussed at three stages using appropriate theoretical tools: At first, the steady state conduction data, then the steady state data with natural convection contribution and, finally, the transient conduction data. The analysis of the results revealed some interesting issues regarding natural convection in microgravity.

2. Experimental procedure and results

The experiments are conducted during the 49th ESA (European Space Agency) Parabolic Flight Campaign which consists of ninety three parabolas split in three days. Each parabola provides a sequence of normal-high-low-high-normal gravity phases. Data of onboard gravitational acceleration provided by ESA showed that during the low gravity phases the gravity value fluctuates randomly (g-jitters) within $\pm 2.6 \times 10^{-2}$ g whereas during the high gravity phases reaches a peak value of about 1.6–1.8 g. The low gravity duration is slightly different among parabolas but on the average lasts approx. 22 s. Each parabola is used to conduct a separate run.

The core of the equipment is a thermostat unit, a CPF-2 type, into which an exchangeable sample cell unit is inserted. The thermostat operates under the gradient reduction principle and can provide precise temperature stability in the order of ±0.05 °C. In addition, the thermostat is equipped with optical and electronic interfaces which enable the stimulation and observation of the test fluid. A sample cell unit is essentially a sealed tube the lower part of which is made of special spectrometer glass cuvette with an internal diameter of 1.5 cm. The cells are specially designed to maintain their measuring chamber (glass cuvette) completely full with liquid in all times so as to prevent free float of the liquid in microgravity. The liquid volume in the cell is approx. 27 cm^3. The pressure inside the cells is kept at ambient values by means of an elastic membrane sealing a port of the cell. Four different cells, filled with a different liquid every time, are used in the present experiments. A detailed schematic of the equipment can be found in [11].

This work presents heating runs conducted with a NTC thermistor (Thermometrics, Inc., 0.125 mm nominal diameter) serving as a local miniature heater. The thermistor (henceforth: the heater) is an axisymmetric ellipsoid with a small-to-large radii ratio of 1:2; the value of the nominal radius represents the two small, approximately equal, radii. In each test cell, the driving electrical circuitry is connected with the heating thermistor by two wires covered with an insulating glass layer. Each insulated wire has a diameter around 0.100 mm. The insulated wires only slightly affect the heat transfer domain around the heating thermistor (more below) so their existence is ignored in the theoretical analysis of the problem.

Fig. 1 shows a 2D schematic of the heater along with some basic features which are important for the theoretical analysis at a subsequent section. The domain V_1 refers to the region of the internal ohmic resistance where actually heat is generated. The domain V_2

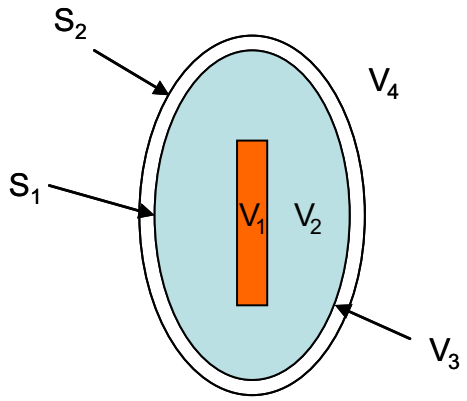

Fig. 1. Geometry of a thermistor (heater).

is the rest of the inner heater consisting of platinum alloy, the domain V_3 is the outer part of the heater consisting of quartz (thickness 10 μm) and the domain V_4 represents the liquid that surrounds the heater. The platinum alloy-quartz interface is denoted as S_1 and the quartz-liquid interface as S_2.

A prescribed voltage value, V_o, is applied to the heater through a special electrical circuitry. V_o is constant through each run but different among runs. Registering the voltage drop V_R across the heater with a sampling frequency of 100 Hz, allows the delivered power and temperature of the heater to be calculated. This is done as follows. The current in the electrical circuitry is given as $I = V_o/(R_t + R_1)$ where R_t is the internal ohmic resistance of the heater and R_1 is a reference constant resistor of the circuitry across which voltage drop is measured. The voltage difference V_R at the edges of R_t is given as

$$V_R = V_o - IR_1 = V_o\left(1 - \frac{R_1}{R_1 + R_t}\right) \tag{1}$$

The resistance R_t can be found by solving the above equation for R_t. The power P delivered by the heater is a function of R_t ($R_t = R_t(T_t)$) from the calibration of each heater against known temperature values):

$$P = V_R I = V_o^2\left(1 - \frac{R_1}{R_1 + R_t}\right)\left(\frac{1}{R_1 + R_t}\right)$$
$$= \frac{V_o^2}{R_1}\left(1 - \frac{1}{1 + R_t(T_t)/R_1}\right)\left(\frac{1}{1 + R_t(T_t)/R_1}\right) \tag{2}$$

The heater temperature is estimated by inverting the function $R_t(T_t)$.

Fig. 2 shows the dimensionless quantity PR_1/V_o^2 versus the heater temperature T_t for the employed four different heaters (sample cells with different thermistors) to give an idea about the temperature dependence of heat generation. The released heat is proportional to the square of the voltage difference V_o and follows a parabolic temperature dependency with a maximum between 80 and 90 °C. This was designed so, because the main objective was to measure natural convection in water at high liquid temperature (max. driving force) yet below its boiling temperature, i.e. 95 °C at 0.83 atm inside the airplane. The curves in Fig. 2 are the characteristic curves of the thermistors resulting from the analysis of the electric circuitry connecting each thermistor. As such, they do not depend on the environment where a thermistor is located. It must be stressed that the whole span of these parabolic power-temperature curves is taken into account in the analysis of the thermistors' temperature evolution.

The thermal performance of the equipment is supervised by a custom-made software. De-ionized water, and glycerol, (BDH Laboratories supplies) are the examined test liquids. Test liquids are initially degassed by boiling at low pressure for one hour. Next, the degassed liquids are used to fill the sample cells. A thermally regulated storage cabinet, part of the flight apparatus, is used to maintain the test cells at a temperature slightly below the temperature of the experiments, 32 °C. The latter was selected for thermal regulation convenience: above the cabin temperature which occasionally may climb to 29 °C.

A brief outline of the experimental scenario is as follows. An exchangeable test cell is inserted in the thermostat and is left to equilibrate at a temperature a few tenths of a degree below 32 °C (considered as the equilibrium temperature T_o). Then the temperature of the liquid is raised locally by energizing the heater at a preset voltage level and for a variable duration. This is usually done about 7 s after the onset of the low gravity phase during a parabola to ensure that the experiment would start at good low gravity conditions. In some runs, the duration of heating is extended inside the succeeding high gravity and normal gravity periods. In a few other runs, heating is started during the high gravity period prior to the low gravity phase. Each test cell is exchanged with a new one after five or ten consecutive parabolas. Due to the initial degassing of test liquids no bubbles appear at any heating run. This is confirmed by optical monitoring of the surface of the heater with a CCD color camera (1k × 1k pixels, 24-bit resolution) but also by the fact that we have never observed the characteristic voltage drop at the heater typical of a growing bubble [11].

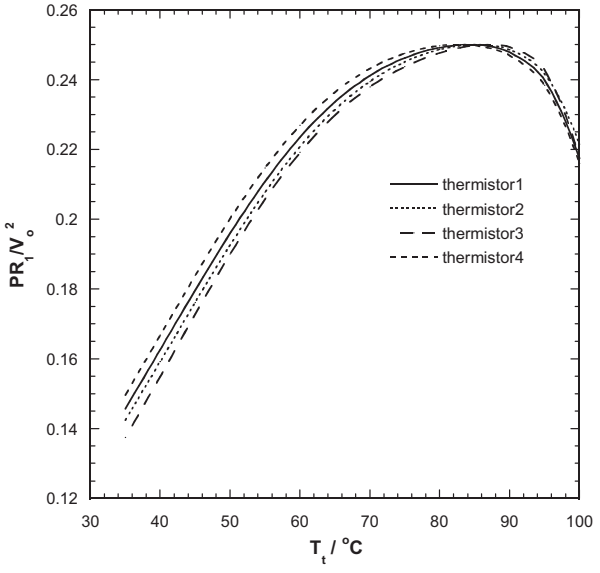

Fig. 2. Dimensionless heat source in the thermistor vs thermistor temperature for the employed four thermistors (heaters).

3. Results and discussion

Figs. 3 and 4 display heater temperatures versus heating time for water and glycerol, respectively, at different applied voltages. Repeatability runs practically coincide so only single runs are presented. A common pattern is found in all heating runs. Temperature climbs very fast at the beginning but only gradually later towards a plateau (steady state) value which, however, is not fully reached in the available heating time. This gets better as the applied voltages get smaller; at voltages below 10.0 Volts in water the steady state is not far from the initial temperature, T_o, and is approached very fast. According to Fig. 2, the fast initial thermalization of the heater is accompanied by a rapid increase of the

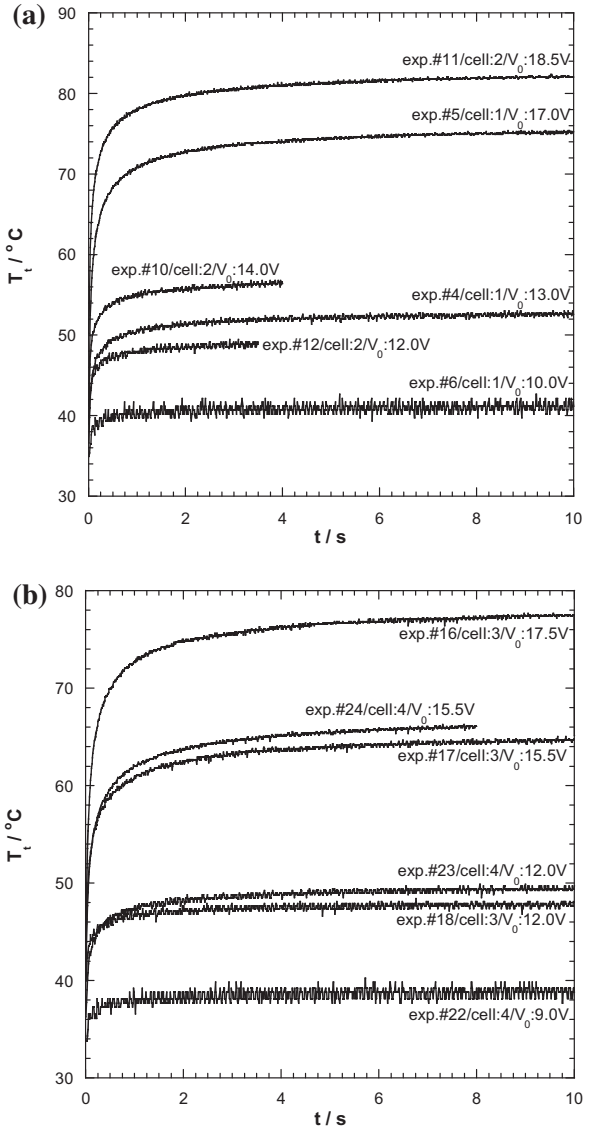

Fig. 3. Heater temperature vs heating time measured for water at different applied voltages: (a) cells 1 and 2, (b) cells 3 and 4.

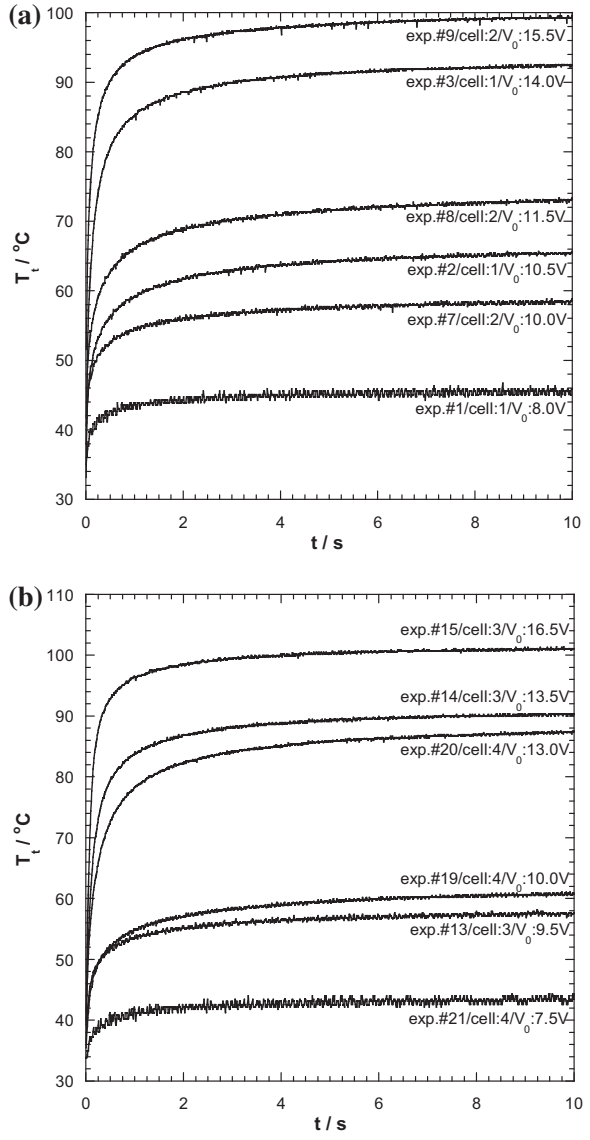

Fig. 4. Heater temperature vs heating time measured for glycerol at different applied voltages: (a) cells 1 and 2, (b) cells 3 and 4.

delivered power. Table 1 summarizes the range of the applied voltages for the two test liquids together with the achieved final temperature and final power (at the end of heating).

Fig. 5 presents a few runs in water and glycerol where heating lasts 50 s. In these runs, heating starts (as in all other cases) from the low gravity phase of a parabola, continues along the entire subsequent high gravity phase and eventually spans a few seconds in the final recovery phase of the parabola where gravity returns to the normal 1 g value. In the three higher power (applied voltage) runs in water (Fig. 5a), the heater temperature is sensitive to changes in gravity level. In particular, going from nearly zero gravity to hypergravity the heater temperature drops. The extent of this drop and the rate it is done depends on heating power and therefore temperature; at higher power (and temperature) the drop is larger and faster. Going from the hypergravity period to normal gravity leads also to an increase of heater temperature which, however, is much smaller than in the low-g/high-g transition. This is rather expected because going from 10^{-2} to 1.8 g is about a 100-fold variation whereas going from 1.8 to 1 g is only a 1.8-fold variation. For the run with the lowest power there is no detectable effect of gravity level on the heater temperature. The latter holds also for the runs with glycerol (Fig. 5b) where the gravitational variations during parabolas did not give any measurable effect. In fact, glycerol was selected as a reference test liquid for which no natural convection is expected due to its high viscosity.

The evolution of the heater temperature is a result of the competition between generation of heat on it by ohmic heating and removal of heat from it to the surrounding liquid by conduction and natural convection. Below an effort is made to understand the experimental results using basic theoretical tools and then to analyze them in order to get important quantitative information regarding the phenomenon of natural convection. The whole analysis is guided in every step by the available experimental results. All the needed physical parameters values are found by interpolating tables with their temperature dependence found in the literature.

3.1. On the existence of natural convection

At first, the effect of natural convection on heater's temperature curves will be discussed in a qualitative manner. The experiments

Table 1
Experimental conditions.

Experiment #	Cell number	V_o (Volts)	Liquid	Final temperature (°C)	Final power (W)
1	1	8	Glycerol	46.7	7.9
2	1	10.5	Glycerol	65.6	17.2
3	1	14	Glycerol	92.9	31.9
4	1	13	Water	53.2	23.1
5	1	17	Water	75.4	47.5
6	1	10	Water	42.7	11.4
7	2	10	Glycerol	59.3	14.6
8	2	11.5	Glycerol	74.0	21.5
9	2	15.5	Glycerol	100.0	35.4
10	2	14	Water	57.0	27.8
11	2	18.5	Water	82.5	57
12	2	12	Water	49.5	18.3
13	3	9.5	Glycerol	58.6	13
14	3	13.5	Glycerol	91.4	30
15	3	16.5	Glycerol	101.6	36.2
16	3	17.5	Water	77.7	50
17	3	15.5	Water	65.0	36.8
18	3	12	Water	48.4	17.7
19	4	10	Glycerol	61.6	15.3
20	4	13	Glycerol	88.3	28
21	4	7.5	Glycerol	45.2	6.9
22	4	9	Water	40.2	9
23	4	12	Water	50.0	19.2
24	4	15.5	Water	66.2	38.1

showed, that for glycerol the contribution of natural convection is zero even at ~1.8 g (Fig. 5b). On the other hand, according to Fig. 5a, in water natural convection is not detectable for a heater temperature T_t = 40 °C but has a measurable value (manifested by the change of the heater temperature when the gravity level changes) for experiments having T_t > 60 °C. According to the theory, the natural convection heat transfer coefficient is a function of a single dimensionless number, the Rayleigh number, which is defined as

$$Ra = \frac{\rho^2 c_p \gamma \beta (T_t - T_o) L^3}{k\mu}$$

where ρ is the density of the liquid, c_p is its specific heat capacity, k its thermal conductivity, μ its dynamic viscosity, β its coefficient of thermal expansion, γ the generalized gravitational acceleration and L a characteristic size of the heater (large semiaxis of the spheroid). In order to compute Ra, the temperature at which the physical properties of the liquid will be estimated must be known. This is not a simple matter because the temperature in the liquid varies between T_o and T_t. A common approach to overcome this problem is to use the so-called "film temperature" $T_f = (T_o + T_t)/2$ (in some cases the suggested weights of T_o and T_f can be different than 0.5). Although this approach is quite successful for the case of water for which a threefold viscosity variation occurs between 30 and 100 °C, it is questionable for the case of glycerol for which the corresponding viscosity variation is 45-fold. We insist here on viscosity because it is much more sensitive on temperature variations than the other physical properties.

The viscosity of glycerol between 100 and 30 °C exceeds 5 to 1000 times the viscosity of water (at 30 °C), respectively. The Ra number is computed for glycerol and water, in Figs. 6 and 7 respectively, using three values of the characteristic temperature T_c for physical property computation, i.e. T_o, T_f and T_t. It is evident that Ra is very sensitive to the choice of T_c. Especially for the case of glycerol the difference may be an order of magnitude. Theoretical correlations for natural convection have been derived using uniform properties (computed at a characteristic temperature T_c) or properties computed at T_o and T_t but the sensitivity of Ra number on temperature shown here suggests that natural convection theories accounting for the variation of physical properties in the liquid domain are necessary.

Given the insufficient knowledge of the problem of natural convection when viscosity exhibits very high sensitivity to temperature, not many things can be said about glycerol. The relevant Ra number of the present experiments can be from 1 to 30. Values around 1 may be compatible to the observed absence of natural convection (since many correlations quote a low limit of validity at Ra = 1 and their uncertainty for Ra < 1 can justify the observed negligible effect of natural convection) but values of 30 certainly not. Of course, rules may be different for the case of highly temperature depended physical properties than the case of uniform properties.

The situation is different for water. In Fig. 7 it is seen that for T_t = 46 where no natural convection is observed experimentally the Ra number varies from 25 to 50 depending on the assumed T_c. According to existing correlations these Ra numbers correspond to significant natural convection. The present experiments indicate clearly that there is a threshold Ra number, Ra_{thr}, below which natural convection is a negligible heat transfer mechanism.

Although there is no measurable heat transfer effect driven by natural convection for glycerol at any of the examined temperatures as well as for water at $T_t \leqslant 46$ °C, it is not clear if this holds also for water at higher T_t. In this case, natural convection appears at 1.8 g so it is possible that it may exist to smaller extent at low gravity due to the g-jitters. The average absolute magnitude of g-jitters in the present experiments is about 0.02 g. Although g-jitters are high frequency variations with alternating sign that do not have time to reach steady state, they are still capable of influencing heat transfer. This means that the Rayleigh number (on $T_c = T_f$ basis, using the appropriate scaling) at low gravity for the experiment at the highest employed temperature is 6, a value much smaller than 37, (see Fig. 7. for T_t = 46 °C), for which no natural convection is observed.

It is important to notice that according to existing correlations for natural convection, there should be an observable contribution

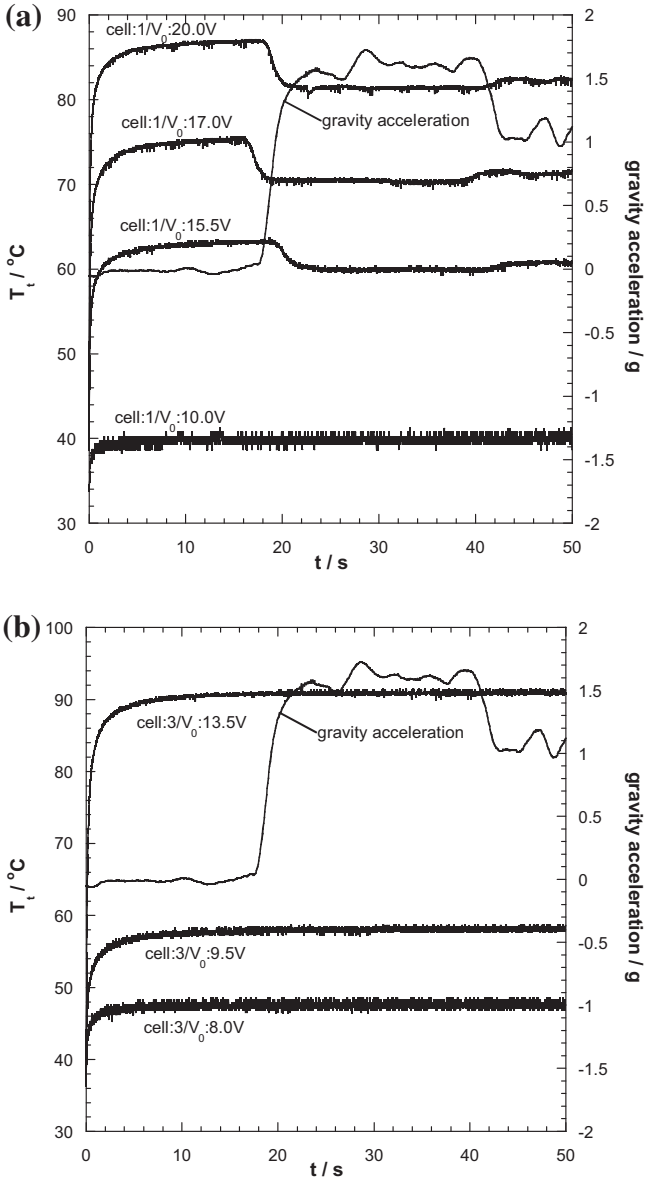

Fig. 5. Evolution of heater temperature and gravity acceleration vs heating time at different applied voltages (a) for water (b) for glycerol.

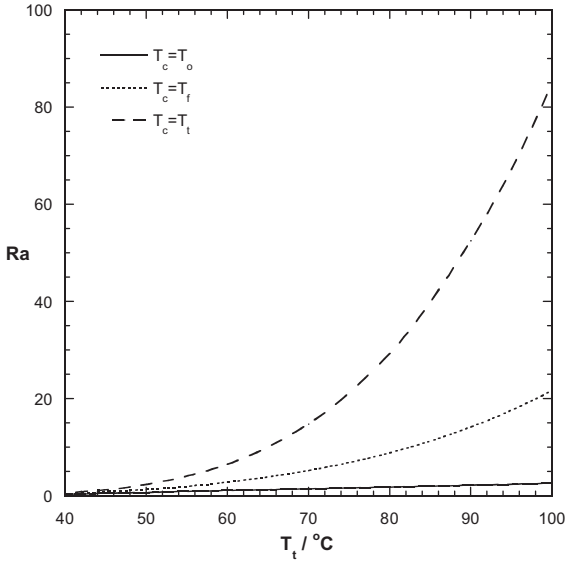

Fig. 6. Computed Ra number vs temperature of heater for glycerol, using three values of the characteristic temperature T_c for physical property computation i.e. T_o, T_f and T_t.

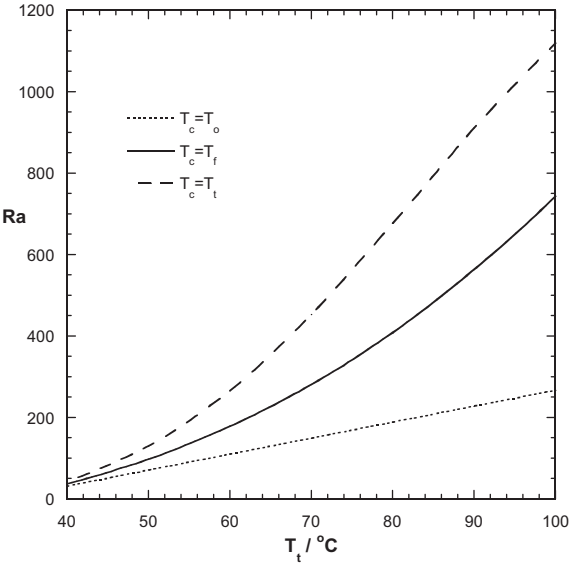

Fig. 7. Computed Ra number vs temperature of heater for water, using three values of the characteristic temperature T_c for physical property computation, i.e. T_o, T_f and T_t.

of natural convection due to such g-jitters. On the contrary the present experiments indicate the existence of a threshold Rayleigh number above which only natural convection heat transfer effects are non-negligible. In other words, in our experiments conducted at low gravity conditions heat transfer occurs solely by conduction.

3.2. Steady state analysis for $Ra < Ra_{thr}$: Pure heat conduction regime

Having shown that the only mechanism of heat transfer at low gravity is conduction we shall try now to explain the experimentally determined steady state temperatures shown in Table 1. At steady state the temperature of the heater fulfills the equilibrium condition

$$P(T_t) = Q(T_t) \tag{3}$$

where P is the power generated at the heater and Q denotes the conduction heat losses from the heater to the liquid. It is noted that the above condition corresponds to a pseudo-steady state since the liquid temperature increases during heating. An elementary heat balance yields that for heat power 30 mW the increase of the average liquid temperature in 20 s is less than 0.02 K so Eq. (3) (based on pseudo-steady state hypothesis) is valid for the time scale of the present experiments.

The next step is to estimate the conduction heat losses from the heater. The heater consists of an inner metallic body with thermal conductivity k_m inside which the heat source is located, and a thin protective layer of thickness δ with thermal conductivity k_q made of quartz. The thermal conductivity k_m of the metallic part is more than 100 times higher than that of the quartz and the liquid so the temperature can be assumed uniform in the inner body of the heater (T_t). The quartz film is thin with respect to the curvature radius of the heater so it can be assumed to be planar. The heat flux through this film is given as

$$\frac{Q_1}{A} = \frac{k_q}{\delta}(T_t - T_i) \tag{4}$$

where A is the surface area of the heater and T_i its outer surface temperature.

In order to determine the heat losses from the outer surface of the heater to the liquid, the Laplace equation for the Dirichlet problem in the exterior domain of a prolate spheroid must be solved. The actual boundaries of the experimental container are too far (about 80 diameters) from the heater so they do not have any influence and an infinite domain can be considered. Fortunately, the particular problem at hand can be solved analytically in prolate spheroidal coordinates. The expression for the rate of heat transferred from the heater to the liquid is [13]

$$Q_2 = \frac{4\pi\sqrt{\alpha^2 - b^2}k(T_i - T_o)}{\ln(\coth(\eta))} \tag{5}$$

where α, b are the large and the small semiaxes of the heater and

$$\eta = \frac{1}{4}\ln\left(\frac{\alpha + b}{\alpha - b}\right) \tag{6}$$

Under steady state conditions it should be $Q_1 = Q_2$. This equation can be solved for T_i which is replaced in Eq. (5) to give the final expression for the conduction heat losses of the heater:

$$Q = \left(\frac{\ln(\coth(\eta))}{4\pi\sqrt{\alpha^2 - b^2}k} + \frac{\delta}{Ak_q}\right)^{-1}(T_t - T_o) \tag{7}$$

where the surface area of the prolate spheroid is computed as:

$$A = 2\pi\left(b^2 + \frac{\alpha b \arccos(b/\alpha)}{\sin(\arccos(b/\alpha))}\right) \tag{8}$$

Substituting the expressions (2) and (7) in (3), a non linear equation arises for the steady state temperature of the heater. Instead of solving for T_t using thermal conductivities values from literature, the experimental steady state temperatures are employed in order to estimate the thermal conductivity of the liquid for each experiment. The estimated conductivities for water and glycerol for all experiments are shown versus the corresponding steady state heater temperature in Fig. 8. In addition, the literature thermal conductivity–temperature curves for the two liquids are shown. In general, the estimated thermal conductivities are very close to literature values. The fluctuation shows a stochastic part which can be attributed to experimental noise (e.g. from the electronics) and a systematic part (most of the experimental data are above the literature curves) which can be attributed to the assumptions made: e.g. ignoring the effect of the finite size of the connecting wires of the heater in the thermal domain, assuming a perfectly spheroidal shape of the heater, assuming that the temperature at the end of the experiment is the steady state one.

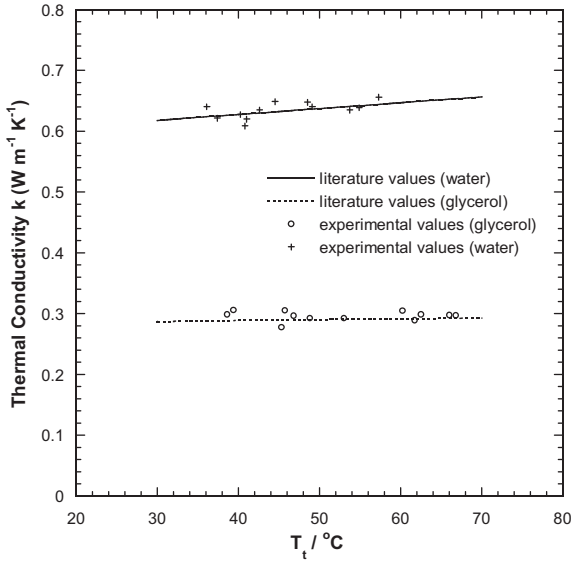

Fig. 8. Thermal conductivities of water and glycerol, estimated from the steady state temperatures of the heater, compared to literature values.

3.3. Steady state analysis for $Ra > Ra_{thr}$: Onset of natural convection

Having analyzed the experimental data for the case of pure heat conduction it is attempted now to derive quantitative information for the magnitude of natural convection employing the experiments with gravity transition from low gravity (no detectable natural convection according to previous section) to ~1.8 g. For Ra numbers smaller than 1000, which is the case for the present experiments, the flow around the heater is strictly laminar. Many relations can be found in the literature for the external heat transfer around an object immersed in an infinite liquid domain regarding laminar natural convection [14,15]. Although in some cases a generalized Churchill interpolation [16] is employed to connect the conduction and natural convection regimes, in practice the interpolation parameter is such that a simple linear addition can be safely assumed. So, the general correlation for the Nusselt number given in literature has the form:

$$\mathrm{Nu} = C_1 + C_2(\mathrm{Pr})\mathrm{Ra}^{1/4} \tag{9}$$

where the parameter C_1 stands for the contribution of conduction and the parameter C_2 depends on Pr number. From the above relation it is expected that the ratio H of natural convection to conduction heat losses from the heater should have the form $H = C(\mathrm{Pr})\mathrm{Ra}^{1/4}$. It must be stressed that a threshold Ra number for the onset of natural convection (similar to the well known one for the case of a restricted liquid domain, e.g. Benard problem [17]) has never been reported in literature for the external heat transfer problem in an infinite domain. The lower limits for Ra number (between 1 and 10) given with the correlations have to do with the accuracy of the corresponding correlation and not with the onset of natural convection.

The ratio H can be estimated from the experimental steady state temperature at ~1.8 g given in Fig. 5a. In particular these temperatures are substituted in the equation

$$P(T_t) = Q(T_t) \tag{10}$$

where the heat losses account now also for natural convection:

$$Q = \left(\frac{\ln(\coth(\eta))}{4\pi\sqrt{\alpha^2 - b^2}k(1+H)} + \frac{\delta}{Ak_q}\right)^{-1}(T_t - T_o) \tag{11}$$

The above equation is solved for H which is shown in Fig. 9 versus the Ra number computed at the surface temperature T_i. The equation for C_2 proposed in literature (C_3 is a constant depending only on the shape of the object) is:

$$C_2 = \frac{0.681C_3}{\left[(1 + 0.492/\mathrm{Pr})^{9/16}\right]^{4/9}} \tag{12}$$

This relation reveals that at the temperature range of the experiments, C_2 is close to constant so a power law with exponent ¼ is expected to relate H with Ra. For a prolate spheroid with the shape of the heater it is $C_1 = 1.759$, $C_2 = 0.948$ [10]. It is clear from the experimental data that the above power law does not hold. Instead of a simple power law we were able to describe the experimental data for H through a generalized power law of the form:

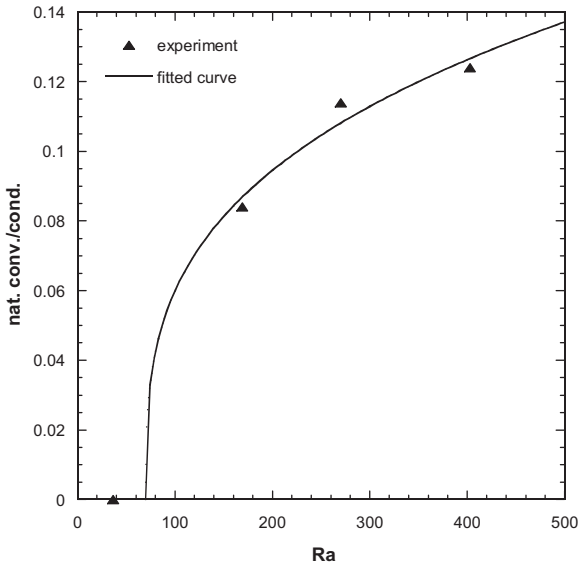

Fig. 9. Ratio of natural convection-to-conduction contribution to heat transfer H vs Rayleigh number. Experimental points and fitted curve in water.

$$H = 0 \quad \text{for Ra} < 70. \tag{13a}$$

$$H = 0.0208^{*}(\text{Ra} - 70)^{0.311} \quad \text{for Ra } 70. \tag{13b}$$

Apparently, the Nusselt number correlation for natural convection derived from the present experiments will have a similar form. The observed temperature changes when the gravitational acceleration goes from ~1.8 to 1 g are too small (given their measurement accuracy) to be able to act as additional confirmation of the above relation but, in general, they are compatible with it.

The present results indicate the existence of a threshold Ra number for the onset of natural convection. In [18] it was shown that the wake developed by the heated object has a size inversely proportional to the Grashof number which implies that for sufficiently small Rayleigh, natural convection may interfere with remote solid walls. This, in turn, implies that there may be an effect of the finite size of test cells in the observed temperatures. In our case this includes also possible effects of the electrical wires connected to the heater. So correlations for natural convection in open geometries should always be accompanied by detailed spatial conditions. In any case, the necessity of further experimental and theoretical study of external natural convection heat transfer for small Rayleigh number is evident. Theoretical studies for modulated gravitational acceleration in closed geometries have been done for relatively large Rayleigh number in order to observe the resulting flow [19] but they can not say anything about the problem considered here.

3.4. Analysis of transient conduction for $Ra < Ra_{thr}$

At this section the focus is on transient heater temperatures when only pure conduction is present. A more detailed modeling approach is required in this case.

The following transient heat conservation equation must be solved in this composite domain:

$$\rho c_p \frac{\partial T}{\partial t} = \nabla k \nabla T + S \tag{14}$$

where the source term, S, is non-zero only in the V_1 domain and the physical properties ρc_p and k are different in each domain. The conventional temperature and heat flux continuity conditions must hold at the interfaces between regions. The initial condition is $T = T_o$ everywhere and the boundary condition far-field in the liquid is $T = T_o$. Although the numerical solution of the above problem is straightforward using an appropriate code, here the derivation of an approximate semi-analytical solution is attempted which permits better insight in the structure of the problem.

The first simplification step arises from the fact that thermal conductivities in domains V_1 and V_2 are similar to each other and much larger than thermal conductivities in domains V_3 and V_4 (by more than 100 times). This results in a uniform temperature profile in regions V_1 and V_2. The evolution equation for the corresponding uniform temperature T_t can be found by taking the volume integral of Eq. (15) for V_1 and V_2 regions and applying Gauss theorem:

$$V_s \rho_s c_{ps} \frac{\partial T_t}{\partial t} = P(T_t) + \int_{S_1} k_q \frac{\partial T}{\partial \vec{n}} ds \tag{15}$$

where the subscript s stands for the properties (volume V_s, density ρ_s and specific heat capacity c_{ps}) of the inner part of the heater, $\vec{n}$ is the outwards normal at the surface S_1 vector. The above equation requires the knowledge of the transient temperature field in the V_3 (quartz) region. A simple estimation of the characteristic heat transfer time in the quartz region leads to a value (from $\tau = \delta^2/\alpha_q$ where δ is the thickness and α_q is the thermal diffusivity of quartz) of the order of 0.001 s. This time scale is very fast to be of interest for the evolution of the measured temperature T_t so it can be assumed that the domain V_3 has a quasi-steady state temperature profile. The solution of the Laplace equation in this domain degenerates to Eq. (17) where T_i is the temperature at the surface S_2. This temperature can be assumed uniform due to the small ratio of the thickness δ to the radius of curvature of the heater

$$T_i = T_t + \frac{\delta}{k_q A} \int_{S_2} k_l \frac{\partial T}{\partial \vec{n}} ds \tag{16}$$

where the equality $\int_{S_1} k_q \frac{\partial T}{\partial \vec{n}} ds = \int_{S_2} k_l \frac{\partial T}{\partial \vec{n}} ds$ is used. This equality is derived by using the pseudo-steady state condition for the quartz region and the heat flux continuity at S_2 surface. So far, there was no need for solving the heat transfer equation in the domains V_1, V_2 and V_3. This is not possible for the domain V_4 for which the equation must be solved in the exterior of a spheroid with a surface temperature $T_i(t)$. Although the steady state heat transfer equation is separable in the prolate spheroidal coordinate system, this is not the case for the transient heat transfer equation. The following approximate technique is used. At first the physical properties of the fluid are assumed to have a constant value in the fluid region during each experiment despite the temperature evolution. This value is taken as the average temperature between T_o and the steady state temperature for the particular experiment. Given the relatively slight variation of thermal conductivity with temperature, the error of this approximation is small.

Let's assume that the heater is spherical with radius R. If $f(t) = T_i(t) - T_o$ then the temperature field in the liquid is given from direct superposition of the Green functions for spherical geometry as follows (r is the radial coordinate and α_w is the thermal diffusivity of the liquid) [20]:

$$T = T_o + \frac{R}{r} \int_{t'=0}^{t} f(t') \frac{r - R}{\sqrt{4\pi\alpha_w}(t - t')^{3/2}} e^{-\frac{(r-R)^2}{4\alpha_w(t-t')}} dt' \tag{17}$$

This form of the solution is not appropriate for the computation of the surface heat flux since the integrand is undefined at $r = R$. To overcome this difficulty an integration by parts taking into account that in the present case $f(0) = 0$, leads to:

$$T = T_o + \frac{2R}{\sqrt{\pi} r} \int_{t'=0}^{t} \left(\frac{df}{dt'}\right) \int_{\xi=\frac{r-R}{2\sqrt{\alpha_w(t-t')}}}^{\infty} e^{-\xi^2} d\xi dt' \tag{18}$$

Despite the double integral this expression is handled easier than Eq. (18) and gives:

$$-\left(\frac{\partial T}{\partial r}\right)_{r=R}=\frac{f(t)}{R}+\frac{1}{\sqrt{\pi\alpha_w}}\int_{t'=0}^{t'=t}\left(\frac{df}{dt'}\right)\frac{1}{\sqrt{t-t'}}dt \tag{19}$$

Multiplying by the surface area of the sphere and the thermal conductivity of the liquid the following relation for the transient heat loss from the sphere to the liquid is obtained:

$$Q_R=Q_{Rs}\left(1+\frac{R}{(T_i-T_o)\sqrt{\pi\alpha_w}}\int_{t'=0}^{t'=t}\left(\frac{df}{dt'}\right)\frac{1}{\sqrt{t-t'}}dt\right) \tag{20}$$

where Q_{Rs} is the well-known (pseudo)steady state heat losses from a sphere ($=4\pi Rk_l(T_i-T_o)$). The integral term is a history integral resulting from the diffusion of the temperature gradients in the fluid temperature field. This term is analogous to the well-known history term accounting for viscosity diffusion in the equation of motion of spheres in fluids [21]. The history term in the more general heat transfer equation from a sphere to a moving fluid was first derived in [22] using Fourier transform and latter in [23]. These authors have shown that its contribution to the transient heat transfer may be significant.

The corresponding relation for the case of a spheroid instead of sphere is obtained by matching the pseudo-steady state terms. In particular, the term for heat losses from a spheroid with temperature T_i

$$Q_{ss}=\left(\frac{4\pi\sqrt{\alpha^2-b^2}k}{\ln(\coth(\eta))}\right)(T_i-T_o) \tag{21}$$

is used in place of Q_{Rs}. The sphere radius R is replaced by the equivalent radius of the spheroid R_s (resulting by matching the two surface areas) which is the characteristic geometrical feature of the particular problem, i.e. $R_s=(A_s/4\pi)^{0.5}$. The whole procedure is similar to putting a singular solution of the transient heat transfer at the center of the spheroid, an approach typically used in low Reynolds number hydrodynamics [24]. The approximate solution is expected to deviate somewhat from the exact solution at small times where the developing temperature front is close to the surface and so the exact shape of the surface is important. When the front has penetrated in the liquid far from the surface (larger times) the shape of the surface is not important and the approximate solution is accurate.

According to the above the approximate equation which must be solved for the temperature of the heater is

$$V_s\rho_s c_{ps}\frac{\partial T_t}{\partial t}=P(T_t)-Q_{ss}\left(1+\frac{R_s}{(T_i-T_o)\sqrt{\pi\alpha_w}}\int_{t'=0}^{t'=t}\left(\frac{dT_i}{dt'}\right)\frac{1}{\sqrt{t-t'}}dt\right) \tag{22}$$

with T_t and T_i related through

$$T_i=T_t-\frac{\delta}{k_q A_s}Q_{ss}\left(1+\frac{R_s}{(T_i-T_o)\sqrt{\pi\alpha_w}}\int_{t'=0}^{t'=t}\left(\frac{dT_i}{dt'}\right)\frac{1}{\sqrt{t-t'}}dt\right) \tag{23}$$

It can be shown that the steady state solution of the above mathematical problem corresponds exactly to the relation (7) previously used for the steady state heat transfer.

The system of the two equations must be solved numerically. It is transformed in a set of algebraic equations by discretizing uniformly the time domain $t_j=jh$ ($j=1,2,3,\ldots$). The discretization of the derivative term is straightforward using the forward Euler method. The integral term includes a singularity in the integrand which is removed using the following discretization scheme (at $t=t_k$):

$$\int_{t'=0}^{t'=t}\left(\frac{dT_i}{dt'}\right)\frac{1}{\sqrt{t-t'}}dt=\sum_{j=1}^{k}\left(\frac{T_j-T_{j-1}}{h}\right)\int_{t_{j-1}}^{t_j}\frac{1}{\sqrt{t_k-t}}dt=\frac{2}{h}\sum_{j=1}^{k}(T_j-T_{j-1})\left(\sqrt{t_k-t_{j-1}}-\sqrt{t_k-t_j}\right) \tag{24}$$

An analytical expression for the transient heat flux from a spheroid to a stagnant liquid was derived in [25] for the case of a spheroid with small eccentricity. The solution is based on the perturbation expansion of the geometry with respect to the eccentricity of the spheroid (up to the second term). In addition to the history term having the same form of the term for a sphere, new more complex history terms appear but it was shown that their practical significance is much smaller than that of the basic history term. Despite the serious arguments against the similarities between the transient heat transfer from spheres and objects with other shapes [26] it is believed that during the approach to steady state the temperature front is far from the heater surface so the exact shape is not important and our approach consists a valid approximation.

The measured and the computed heater temperature evolution curves for heater 1 with glycerol and water are shown in Figs. 10 and 11 respectively, for three different values of input voltage V_o. Similar results are taken for the other heaters. In general, the agreement between measured and theoretical results is very good considering the approximate character of the theory and the accuracy of the measured results. All major features of the experimental curves are reproduced by the theory. Both the fast first stage and the slow second stage of temperature rise are adequately predicted. According to the theory, the approach to the steady state temperature is very slow (asymptotically reached) requiring more than 15 s. Assuming as steady state temperature for the theory the experimental temperature for $t=15$ s (T_{15}) is the reason for the slight discrepancy between theory and experiment at large times i.e. the theoretical curves converge asymptotically to T_{15} whereas the experimental temperature converges asymptotically to a larger value not accessible experimentally. The approach to the

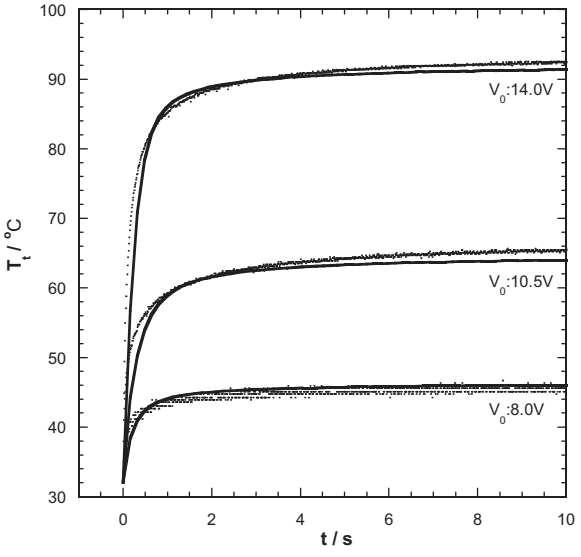

Fig. 10. Comparison between computed and experimental evolution of heater temperature (glycerol, heater: thermistor 1) (solid lines: computed values, dotted lines: experimental values).

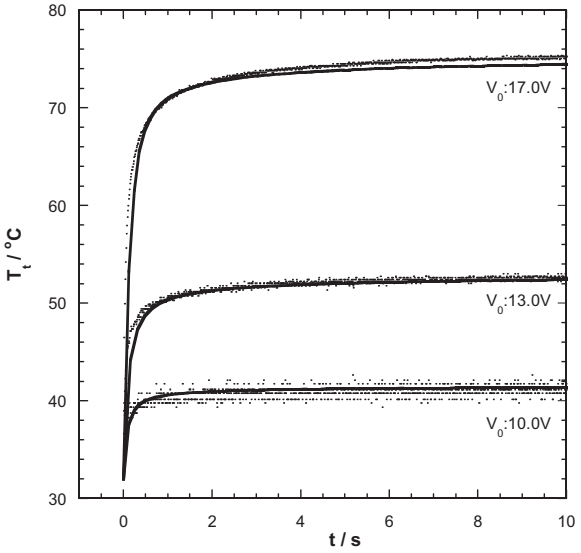

Fig. 11. Comparison between computed and experimental evolution of heater temperature (water, heater: thermistor 1) (solid lines: computed values, dotted lines: experimental values).

asymptotic value is faster for the case of water due to the larger thermal diffusivity of water with respect to that of glycerol.

Despite the agreement between experiment and theory which confirms the conductive nature of heat transfer in the low gravity experiments, the slow convergence to the steady state is still surprising. Specifically, a conduction time scale for the particular problem at hand is $\tau = [(\alpha + b)/2]^2/\alpha_W$ which for the case of water is about 0.16 s. How such a small characteristic time can be associated with a convergence time larger than 15 s? It is reminded than in literature the diffusive field around a sphere is considered to be in steady state for $t \gg \tau$ [27]. Although this argument is valid for the temperature itself, it is not valid for the temperature gradient which approach its asymptote value algebraically according to $Q - Q_{as} \propto \alpha_w (t/\tau)^{-1/2}$. This explains why the conductive time scale is not appropriate to estimate the time scale of convergence of the heater temperature to its asymptotic value. In order to illustrate better the influence of the transient heat conduction in the liquid to the heater evolution temperature, Fig. 12 compares the theoretical curves for glycerol (heater 1 and two values of V_o) with the corresponding curves for pseudo-steady state temperature field in the liquid ($\alpha_W \to \infty$). In this case the temperature converges to its steady state exponentially with characteristic time τ. The Figure confirms that the slow second stage of the heater temperature rise is neither due to the thermal capacity of the heater, nor due to the non-linear relation between the heat source and the temperature and is not an experimental artifact. This stage corresponds to the dynamics of heat conduction in a semi-infinite domain.

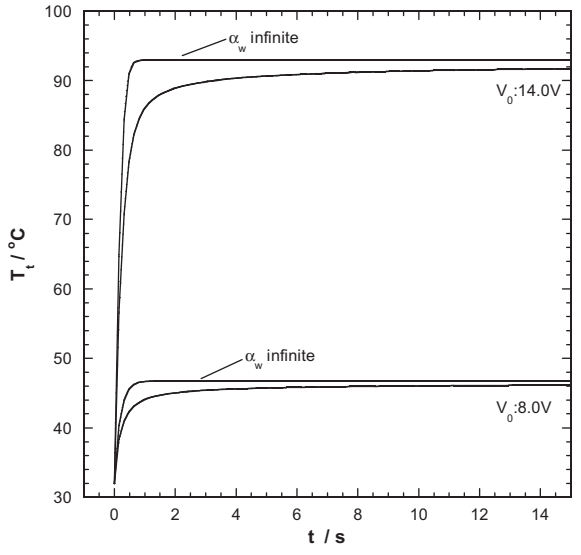

Fig. 12. Computed evolution of heater temperature in glycerol compared to the case of infinite thermal diffusivity of liquid.

4. Conclusions

In the present work several experiments were performed in water and glycerol where the temperature evolution of a sub millimeter size spheroid heater with a temperature dependent heat source was recorded at low gravity. The primary scope was to study the influence of residual g-jitters on the heat transfer from the heater to the surrounding liquid. The results showed that a minimum (threshold) Rayleigh number is required for natural convection to yield a measurable contribution to heat transfer process (contrary to predictions of existing theories and correlations for external geometries). This means that there is practically no influence of g-jitters on heat transfer and the only heat transfer mechanism for miniature heaters at low gravity conditions is pure conduction. Using only conduction terms, an approximate mathematical model is developed for the transient heat transfer problem in the experimental set up which describes the experimental data sufficiently well. This is an additional confirmation that the only heat transfer mechanism at low gravity is conduction.

Acknowledgments

We are thankful to European Space Agency for kindly providing the parabolic flights (ESA PS-49/50E/2007-5/VP). Also, the financial support by ESA through the project CBC (Convective Boiling and Condensation: local analysis and modeling of dynamics and transfers, ESA-AO-2004-PCP-111/ELIPS-2) is gratefully acknowledged.

References

[1] B. Gebhart, Y. Jaluria, R.L. Mahajan, B. Sammakia, Buoyancy Induced Flow and Transport, Hemisphere Publishing Corporation, New York, 1988.
[2] W.M. Deen, Analysis of Transport Phenomena, Oxford University Press, London, 1998.
[3] M. Molla, A. Hossain, M.C. Paul, Natural convection flow from an isothermal horizontal circular cylinder in presence of heat generation, Int. J. Eng. Sci. 44 (2006) 949–958.
[4] T. Cebeci, P. Bradshaw, Physical and Computational Aspect of Convective Heat Transfer, Springer-Verlang, New York, 1984.
[5] F.E. Fendell, Laminar natural convection about an isothermally heated sphere at small Grashof number, J. Fluid Mech. 34 (1968) 163–176.
[6] C.A. Hieber, B. Gebhart, Mixed convection from a sphere at small Reynolds and Grashof numbers, J. Fluid Mech. 38 (1969) 137–159.
[7] T. Sano, Unsteady natural convection about a sphere at small Grashof number, Phys. Fluid. 25 (1982) 2204–2206.
[8] S. Shafie, N. Amin, I. Pop, The effect of g-jitter on double diffusion by natural convection from a sphere, Int. J. Heat Mass Transfer 48 (2005) 4526–4540.
[9] S. Shafie, N. Amin, g-Jitter induced free convection boundary layer on heat transfer from a sphere with constant heat flux, J. Fund. Sci. 1 (2005) 44–54.
[10] W.M. Rohsenow, J.M. Hartnett, Y.I. Cho, Heat Transfer Handbook, Mc Graw Hill, New York, 1998.
[11] N. Divinis, T. Karapantsios, R. de Briyin, M. Kostoglou, V. Bontozoglou, J. Legros, Bubble dynamics during degassing of dissolved gas saturated solutions at microgravity conditions, AIChE J. 52 (2006) 3029–3040.
[12] M. Kostoglou, T.D. Karapantsios, Bubble dynamics during the non-isothermal degassing of liquids Exploiting microgravity conditions, Adv. Colloid Interface Sci. 134-135 (2007) 125–137.
[13] P. Moon, D.E. Spencer, Field theory for engineers, Van Nostrand Company, New York, 1961.
[14] A. Campo, Correlation equation for laminar and turbulent convection from spheres, Warme- und Stoffubertragung 13 (1980) 93–96.

[15] S.W. Churchill, R. Churchill, A comprehensive correlating equation for heat and component transfer by free convection, AIChE J. 21 (1975) 604–606.
[16] S.W. Churchill, R. Usagi, A general expression for the correlation of rates of transfer and other phenomena, AIChE J. 18 (1972) 1121–1128.
[17] P.G. Drazin, W.H. Reid, Hydrodynamic Stability, Cambridge University Press, Cambridge, 1981.
[18] H. Jia, G. Gogos, Laminar natural convection heat transfer from isothermal spheres, Int. J. Heat Mass Transfer 39 (1996) 1603–1615.
[19] M.P. Dyko, K. Vafai, Effects of gravity modulation on convection in a horizontal annulus, Int. J. Heat Mass Transfer 50 (2007) 348–360.
[20] M.N. Ozisik, Boundary Values Problem of Heat Conduction, Dover, New York, 1989.
[21] M.R. Maxey, J.J. Riley, Equation of motion of a small rigid sphere in a non-uniform flow, Phys. Fluid. 26 (1983) 883–889.
[22] E.E. Michaelides, Z.G. Feng, Heat transfer from a rigid sphere in a non-uniform flow and temperature field, Int. J. Heat Mass Transfer 37 (1994) 2069–2076.
[23] M.R. Heikal, S.S. Sazhin, V.A. Goldshtein, A transient formulation of Newton's cooling law for spherical bodies, J. Heat Transfer 123 (2001) 63–64.
[24] C. Pozrikidis, Boundary integrals and singularity methods for linearized viscous flow. Cambridge Text in Applied Mathematics, Cambridge, 1992.
[25] Z.G. Feng, E.E. Michaelides, Transient heat and mass transfer from a spheroid, AIChE J. 43 (1997) 609–616.
[26] E.E. Michaelides, Particles, Bubbles and Drops-Their motion, heat and mass transfer, World Scientific Publishing, Singapore, 2006.
[27] S.K. Friedlander, Smoke, Dust and Haze: Fundamentals of Aerosol Dynamics, Second ed., Oxford University Press, New York, 2000.